SEISMIC RANDOM NOISE ATTENUATION USING DIRECTIONAL TOTAL VARIATION IN THE SHEARLET DOMAIN

DEHUI KONG[1], ZHENMING PENG[1], HONGYI FAN[2] and YANMIN HE[1]

[1] *School of Opto-Electronic Information, University of Electronic Science and Technology of China, Chengdu 610054, P.R. China. kongdehui_2007@sina.com*
[2] *Brown University, School of Engineering, 182 Hope Street, Providence, RI 02912, U.S.A. hongyi_fan@brown.edu*

(Received August 31, 2015; revised version accepted May 9, 2016)

ABSTRACT

Kong, D., Peng, Z., Fan, H. and He, Y., 2016. Seismic random noise attenuation using directional total variation in the shearlet domain. *Journal of Seismic Exploration*, 25: 321-338.

In this paper we propose an effective seismic denoising method using directional total variation (DTV) in the shearlet domain. This approach exploits the sparseness of shearlet transform and direction sensitivity of DTV. Shearlet shrinkage has a positive effect on denoising, but suffers from Gibbs artifact which can be solved by total variation (TV). DTV is an improved method of TV using anisotropic projection and performs well for the noisy signal with a dominant direction. The seismic data can be decomposed into several subbands by shearlet transform. Every subband has its own dominant direction. Therefore applying the direction information to DTV can more effectively eliminate seismic noise. The application on synthetic data and field data shows that the proposed method is superior to shearlet transform or DTV in seismogram noise removal and feature preservation.

KEY WORDS: shearlet, directional total variation, sparse representation, seismic random noise attenuation.

INTRODUCTION

As the terrain of seismic exploration becomes more complex, the quality of acquired seismic data may not reach our requirement. The data are often distorted by noise in survey procedure, data recording, etc. In some extreme cases, the valid signal is lost in the noise. In addition, some processes, such as thin layer estimation and AVO inversion (Puryear and Castagna, 2008; Alemie and Sacchi, 2011), have high demands on the quality of seismic record.

0963-0651/16/$5.00

Therefore noise attenuation is a hot continuous topic on seismic preprocessing. Seismic noise can mostly be divided into two parts: incoherent noise (often called white noise) and coherent noise. The noise statistical properties often have an important influence on choosing algorithms (Zhong et al., 2015). In this paper, we concentrate on random noise, which is very common and easily damages the characteristics of seismic data and stratigraphic interpretation. The random noise indicates the incoherent noise in seismic data. It mainly comes from wind motion, recording instruments, etc (Yilmaz, 2001). The random noise processed in this article is an additive noise. It has a fixed variance and its mean is approximately zero. The first and second order statistical moments are time-invariant.

There are two main kinds of incoherent noise suppression, i.e., harmonic analysis and partial differential equations. Harmonic analysis is a powerful tool for dealing with the issue of random noise suppressing. It represents the signal as the superposition of a set of basic waves. Since the effective part has a particular structure and random noise does not have a specific structure, the signal obtained by the decomposition focuses on some basic waves and noise is evenly distributed within each wave. This method can effectively separate the signal and noise components. Then a shrinkage operator is used for each basic component decomposed from the noisy signal. The noise can be suppressed greatly with a proper shrinkage parameter. Finally the denoised result is obtained by synthesizing the processed basic signals. An important factor of the performance of harmonic analysis denoising is the implement tool, for example, Fourier transform, wavelet transform (Shan et al., 2009) and multi-scale analysis (including curvelet transform (Starck et al., 2002), contourlet transform (Do and Vetterli, 2005), shearlet transform (Easley et al., 2008), etc.). If decomposition methods give the more structural characteristics of signal, the converting coefficients are sparser. This sparseness can be regarded as the effectiveness of separation between signal and noise. The reason for selecting shearlet as harmonic analysis tool is its superior ability in sparse representation of seismic wave (Yi et al., 2009).

However, the harmonic analysis has difficulty to recover sharp discontinuities for its direct cutting off. This is shown as some Gibbs artifacts. To suppress the artifacts, a combination with total variation (TV) has attracted many attentions. TV regularization tries to minimize the gradient of the signal in the l_1 norm (Rudin et al., 1992). The combination of harmonic analysis and TV has improved performance of the denoising result (Glenn et al., 2008; Tang and Ma, 2011; Guo et al., 2013; Lari and Gholami, 2014). This method also has its limitation, especially the oil painting artifacts. Many efforts have been made to improve the performance of TV (Bredies, 2010; Bayram, 2012; Benning et al., 2013). In particular, the directional TV (DTV) is a representative one. DTV weights the gradients depending on their direction

features which improve the sensitivity to variation at a selected direction. DTV requires a signal to have a dominant direction characteristic. The real signal has various geometric features and rarely has a single dominant direction feature. Therefore, the noisy signal is firstly decomposed into a set of basic components which have their own characteristics in different directions. Then DTV denoising method is used to process each basic component, achieving better results. The experiments between synthetic data and field data all approve this conclusion.

In the rest of this paper, we start with a review on shearlet transform and DTV in the next section. Then the combination of shearlet transform and DTV is shown in the third section. And the comparison of the proposed method and related algorithms in the simulated and real seismic data processing is present, respectively. Finally we summarize the main results and suggest directions for further work.

THEORY

Shearlet is an excellent tool for sparse representation. It takes advantages of multiscale analysis and a shear operator to capture the geometry of multidimensional data. Each subband from shearlet transform describes a particular direction feature. Using direction characteristic, DTV can effectively suppress random noise. In this section, an introduction of shearlet and DTV is given below.

Shearlet transform

Shearlet transform employs a family of operator on a single function to realize a partition in frequency domain. A shear matrix is applied to obtain direction information while curvelet uses rotation operator in polar domain. Here, **S** is a simple shear matrix:

$$\mathbf{S} = \begin{bmatrix} 1 & s \\ 0 & 1 \end{bmatrix}, \quad s \in \mathrm{R} \tag{1}$$

where R denotes the real number set. Then an anisotropic dilation operator **A** is represented as

$$\mathbf{A} = \begin{bmatrix} a & 0 \\ 0 & \sqrt{a} \end{bmatrix}, \quad a \in \mathrm{R}^{+} \tag{2}$$

where a represents an anisotropic dilation. Shearlet basis is generated by using the previous operators and translation vector on mother wavelet ψ:

$$\psi_{a,s,m}(x) = \psi[\begin{pmatrix} 1 & -s \\ 0 & 1 \end{pmatrix} \times 2^{-2a} \times (x - \mathbf{m})] \quad , \tag{3}$$

where s presents the shear operator in the shear matrix, a is the dilation parameter corresponding to the dilation matrix **A** and **m** is a two dimension translation vector. The basis has a separate form in the frequency domain:

$$\hat{\psi}(\mathbf{w}) = \hat{\psi}_1(w_1)\hat{\psi}_2(w_1/w_2) \quad , \tag{4}$$

$$\hat{\psi}_{a,s,m}(\mathbf{w}) = \hat{\psi}_1(4^{-a}w_1)\hat{\psi}_2[2^a(w_2/w_1) + s]e^{-2\pi i<w,m>} \quad , \tag{5}$$

where **w** is a two dimensional vector, and w_1, w_2 represent the frequency in horizontal and vertical direction, respectively. From the definition of $\hat{\psi}_{a,s,m}(\mathbf{w})$, its frequency support can be shown as Fig. 1.

In Fig. 1a, the basis function $\hat{\psi}_{a,s,m}(\mathbf{w})$ rotates in one level subband through shear parameter .

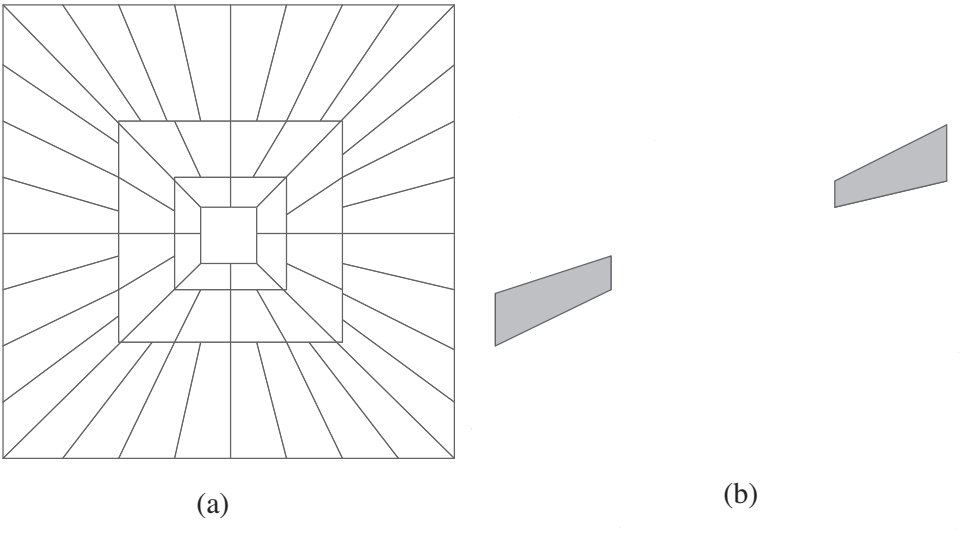

Fig. 1. (a) Partitions of the frequency plane produced by shearlet. The part of support is symmetrical. (b) One of the symmetrical sub-band.

The continuous shearlet transform of a signal $f \in L^2(R^2)$ can be defined as

$$SH_\psi(f)(a,s,m) = \langle f, \psi_{a,s,m} \rangle = \int \int_{R^2} f(\mathbf{x}) \psi_{j,k,m}(\mathbf{x}) d\mathbf{x} \quad . \tag{6}$$

Nature signals usually have many edges and anisotropic features. It is shown that shearlet is essentially optimal in representing a two-dimensional function (Guo and Labate, 2007). The N-term largest reconstruction coefficient f_N^S obtained by shearlet transform can estimate the original function f with an asymptotic approximation error decays as

$$\| f - f_N^S \|_2 \leq N^{-2} (\log N)^3 \ , \quad N \to \infty \tag{7}$$

which is much smaller than that from wavelet CN^{-1}. In this article, shearlet is selected for its directional sensitivity, optimal sparse representation, and easy to implement.

DTV method

Harmonic analysis methods are not perfect because they are often confused by ringing artifacts. Total variation is a powerful tool for denoising and suppressing the ringing artifacts. However, this method suffers from oil-paintings in the case of complex textures and shading. Many efforts have been made to overcome this shortage. DTV is one of the good works. Different from traditional TV, DTV adds direction information to calculate the variation which strengthens the dominant direction component. This model has a higher sensitivity to the direction which is more effective in processing signals with dominant direction.

TV of a discrete signal f(x,y) is defined as

$$\begin{aligned} TV(f) &= \sum_{x,y} \| \nabla f(x,y) \|_2 \\ &= \sum_{x,y} \sqrt{\{[\nabla f_x(x,y)]^2 + [\nabla f_y(x,y)]^2\}} \ , \end{aligned} \tag{8}$$

where ∇f_x and ∇f_y denote horizontal and vertical difference, respectively

$$\begin{aligned} \nabla f(x,y) &= [\nabla f_x(x,y), \nabla f_y(x,y)] \\ \nabla f_x(x,y) &= f(x,y) - f(x-1,y) \\ \nabla f_y(x,y) &= f(x,y) - f(x,y-1) \ . \end{aligned} \tag{9}$$

Tang and Ma (2011), Lari (2014) adopted TV minimization to shrink coefficients. In eq. (8), the TV can be reformulated as a vector inner product

$$TV(f) = \sum_{x,y} \| \nabla f(x,y) \|_2 = \sum_{x,y} \sup\langle \nabla f(x,y), t \rangle \quad , \tag{10}$$

where t is a unit vector in the l_2 norm ball. Let f_x and f_y represent $\nabla f_x(x,y)$ and $\nabla f_y(x,y)$, respectively. Eq. (10) can be extended as

$$\begin{aligned} TV(f) &= \sup\langle (f_x,f_y), r \rangle \\ &= \sup\left\langle (f_x,f_y), \left([f_x/\sqrt{\{f_x^2+f_y^2\}}], [f_y/\sqrt{\{f_x^2+f_y^2\}}] \right) \begin{pmatrix} \cos\theta & \sin\theta \\ -\sin\theta & \cos\theta \end{pmatrix} \right\rangle \\ &= \sup\left\langle (f_x,f_y), \left([(f_x\cos\theta - f_y\sin\theta)/\sqrt{\{f_x^2+f_y^2\}}], [(f_x\sin\theta + f_y\cos\theta)/\sqrt{\{f_x^2+f_y^2\}}] \right) \right\rangle \\ &= \sup\left\langle [(f_x^2\cos\theta - f_xf_y\sin\theta)/\sqrt{\{f_x^2+f_y^2\}}] + [(f_xf_y\sin\theta + f_y^2\cos\theta)/\sqrt{\{f_x^2+f_y^2\}}] \right\rangle \\ &= \sup\left\langle \sqrt{\{f_x^2+f_y^2\}}\cos\theta \right\rangle \quad , \end{aligned} \tag{11}$$

where the operators $\cdot$ and $\langle , \rangle$ represent matrix product and vector inner product, respectively. From eq. (11), the upper bound of TV is obtained when θ equals to zeros. The unit vector $\mathbf{r}$ is $(f_x/\sqrt{\{f_x^2+f_y^2\}}, f_y/\sqrt{\{f_x^2+f_y^2\}})$, i.e., the same direction with TV. The upper bound is not related to the variable θ. So the original TV is isotropic as a consequence of the isotropic unit vector in the l_2 norm ball. When the norm ball is replaced by an anisotropic ellipse, it renders TV the direction sensitivity as shown in Fig. 2a. When TV is projected onto an ellipse to search for an extreme value, the DTV can be represented by the original TV through a rotation matrix $\mathbf{K}_\theta$ and scale matrix $\mathbf{L}_\alpha$.

The mapping between the original TV and DTV is

$$v(i,j)_{v \in E_{\alpha\theta}} = \mathbf{K}_\theta \mathbf{L}_\alpha v(i,j)_{v \in B_2} \quad , \tag{12}$$

where α represents the major axis of the ellipse,

$$K_\theta = \begin{pmatrix} \cos\theta & -\sin\theta \\ \sin\theta & \cos\theta \end{pmatrix}, \quad L_\alpha = \begin{pmatrix} \alpha & 0 \\ 0 & 1 \end{pmatrix}. \tag{13}$$

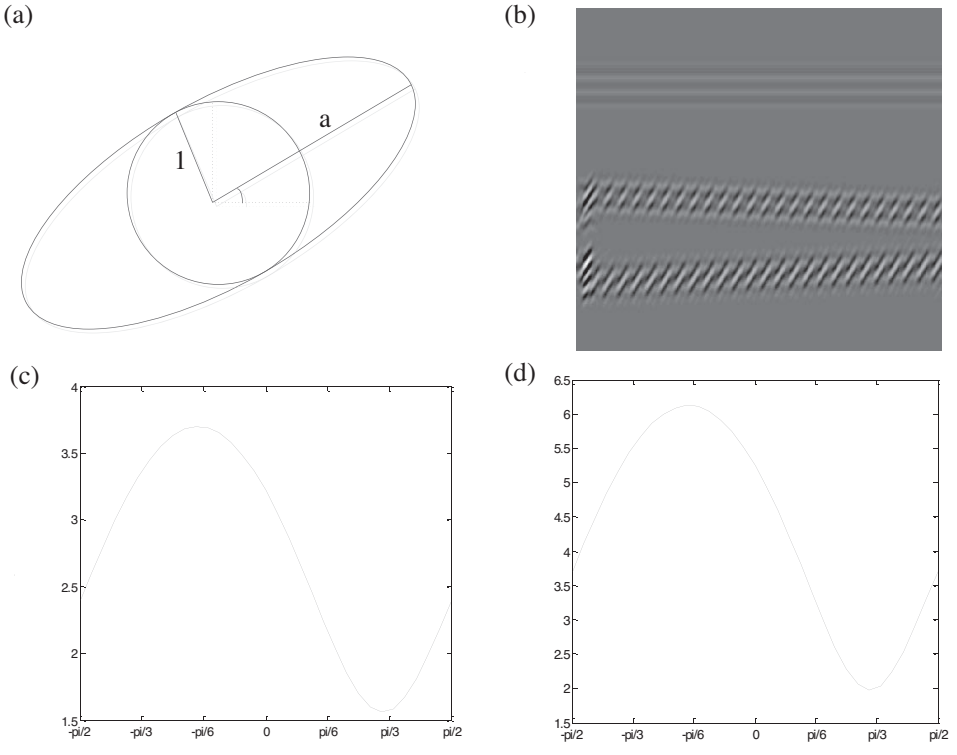

Fig. 2. The direction sensitivity of subband. (a) The projection difference between TV and DTV. (b) A subband from synthetic data. (c) The value of DTV with a = 3. (d) The value of DTV with a = 5.

DTV is computed by the following inner production:

$$
\begin{aligned}
\mathrm{DTV}_{\alpha\theta}(f) &= \sup\langle (f_x,f_y), r(\alpha\theta)\rangle \\
&= \sup\langle (f_x,f_y)\rangle \\
&= \sup\left\langle (f_x,f_y), \left([f_x/\sqrt{\{f_x^2+f_y^2\}}],[f_y/\sqrt{\{f_x^2+f_y^2\}}]\right)\cdot \begin{pmatrix} \alpha & 0 \\ 0 & 1 \end{pmatrix} \cdot \begin{pmatrix} \cos\theta & \sin\theta \\ -\sin\theta & \cos\theta \end{pmatrix} \right\rangle \\
&= \sup\left\langle (f_x,f_y) \begin{pmatrix} \alpha & 0 \\ 0 & 1 \end{pmatrix}, \left([f_x/\sqrt{\{f_x^2+f_y^2\}}],[f_y/\sqrt{\{f_x^2+f_y^2\}}]\right) \begin{pmatrix} \cos\theta & -\sin\theta \\ \sin\theta & \cos\theta \end{pmatrix} \right\rangle \\
&= \sup\left\langle (\alpha f_x^2, f_y^2), r(1,-\theta)\right\rangle \quad . \qquad (14)
\end{aligned}
$$

The final derivation indicates that the upper bound is dependent on θ.

For the anisotropy of ellipse, the minimum can be linked with the direction of TV. Fig. 2b shows a subband by shearlet transform from synthetic seismic record with a dominant direction $\theta = \pi/3$. Its TV value is calculated by projecting onto the ellipses in terms of $\alpha = 3$ and $\alpha = 5$ shown in Figs. 2c-d, respectively. These figures reveal that each subband obtained by shearlet transform has its own dominant direction and DTV can find out the dominant direction. In addition, a bigger α leads to a higher amplitude.

THE PROPOSED METHOD

The condition may be more complex because of the diversity of noise in field data which will be the next work. In this article, we dedicate to the noise in the following model:

$$\mathbf{s} = \mathbf{f} + \mathbf{n} \quad , \tag{15}$$

where $\mathbf{s}$ is the acquired noisy data, $\mathbf{f}$ denotes the noise-free signal to be estimated, and $\mathbf{n}$ is the random noise which is considered as a stationary and Gaussian process. In an ideal case, the noise is Gaussian distributed according to the Central Limit Theorem (Zhong et al., 2015).

As shown in the last section, shearlet transform can be used to obtain direction information of seismogram. Direction of every subband changes regularly as the $\hat{\psi}_{a,s,m}(\mathbf{w})$ rotates with the shear parameter. The proposed method integrates shearlet transform and DTV to reconstruct seismic record with direction features and less distortion.

In order to combine shearlet transform and DTV, the following object function is proposed

$$\mathrm{f}_{\alpha,\theta} = \arg\min_{\mathrm{f}_i} \sum_i \left[\tfrac{1}{2} \left\| \mathrm{SH}_i(\mathbf{s}) - \mathrm{f}_i \right\|_2^2 + \lambda_i \mathrm{DTV}_{\alpha,\theta}(\mathrm{f}_i) \right] \quad , \tag{16}$$

where $\mathrm{SH}_i(\mathbf{s})$ is the i-th subband of the shearlet transform. For computation simplicity, the fast finite shearlet transform (FFST2.0) (Hauser and Steidl, 2013) is adopted for numerical computation. f_i is the corresponding denoised subband. It should be noted that eq. (16) is separable with respect to the subband. Then a simplicity formulation can be reached

$$\hat{\mathrm{f}}_i = \arg\min_{\mathrm{f}_i} \tfrac{1}{2} \left\| \mathrm{SH}_i(\mathbf{s}) - \mathrm{f}_i \right\|_2^2 + \lambda_i \mathrm{DTV}_{\alpha,\theta}(\mathrm{f}_i) \quad , \tag{17}$$

where $\hat{f}_i$ is the result of i-th subband. Taking eq. (12) into consideration, the object function (17) has another description as

$$\hat{f}_i = \arg\min_{f_i} \tfrac{1}{2} \| SH_i(s) - f_i \|_2^2 + \lambda_i K_\theta L_\alpha TV(f_i) \quad . \tag{18}$$

Auxiliary variable u and v are taken to represent the processing subband $SH_i(s)$ and its TV, $TV(f_i)$ respectively. Through the derivation of the variation f_i, the process becomes the optimal problem of v:

$$v = \arg\min_{v \in B_2} \tfrac{1}{2} \| u - \lambda \Delta^T K_\theta L_\alpha v \|_2^2 \quad . \tag{19}$$

Since the function is quadratic, its second order Taylor expansion about point v′ is written as:

$$\begin{aligned} G(v) &= G(v') + (v - v')^T(\lambda\Delta^T K_\theta L_\alpha)^T(\lambda\Delta^T K_\theta L_\alpha v' - u) \\ &\quad + \tfrac{1}{2}(v - v')^T(\lambda\Delta^T K_\theta L_\alpha)^T(\lambda\Delta^T K_\theta L_\alpha)(v - v') \\ &\le G(v') + (v - v')^T(\lambda\Delta^T K_\theta L_\alpha)^T(\lambda\Delta^T K_\theta L_\alpha v' - u) \\ &\quad + \tfrac{1}{2}(v - v')^T D(v - v') \quad , \end{aligned} \tag{20}$$

where D is a symmetric diagonal matrix such that

$$D \ge (\lambda\Delta^T K_\theta L_\alpha)^T(\lambda\Delta^T K_\theta L_\alpha) = \lambda^2\alpha^2\Delta\Delta^T \quad . \tag{21}$$

Because of the positive semi-definite (psd) of matrix $\Delta\Delta^T$, there is a positive scalar ε that makes $\varepsilon I - \Delta\Delta^T$ be a psd matrix where I denotes identity matrix. A choice of D can be $\varepsilon\lambda^2\alpha^2 I$. Under such conditions, an iteration minimization method can be hold by $G(v) \le G(v')$. Inserting the choice into eq.(20), it is written as:

$$G(v) \le (\varepsilon\lambda^2\alpha^2/2) \| v - \psi(v') \|_2^2 + C \quad , \tag{22}$$

where C is an independent constant of v′ and

$$\psi(v') = v' + (1/2\varepsilon\lambda^2\alpha^2)W^T(u - Wv') \quad , \quad W = \Delta^T K_\theta L_\alpha \quad . \tag{23}$$

This means that the new estimation about v has the same formulation with $\psi(v')$. Besides, the element in new result of iteration should satisfy unit ball constraint. This is achieved by a shrinkage operator as:

$$v(x,y) = \begin{cases} v(x,y) & \|v(x,y)\|_2 < 1 \\ v(x,y)/\|v(x,y)\|_2 & \text{else} \end{cases} . \quad (24)$$

The following Algorithm 1 gives a pseudo-code implementation of the proposed method. Other versions can refer to the work of majorization-minimization algorithm (Figueiredo et al., 2007). The number of subbands is set as N in shearlet transform. The variable u_i is used to represent the i-th subband. There are two main steps to deal with every u_i. First, we need to search for a dominant direction θ of the current subband. Then, under the dominant direction, the iteration method for eqs. (23) and (24) is used to suppress the random noise.

Algorithm 1. Seismogram Denoising by DTV in ST

Input: $\mathbf{s}$, α, i, θ, λ, ε, mIter

Output: $\mathbf{s}'$

Initialization: i = 1, θ = 0, v = 0

1: [$\mathbf{u}$,N] = FFST($\mathbf{s}$)

2: repeat

3: for j = 0:π/6:2π

4: subDir(j) = $DTV_{a,j}[SH_i(\mathbf{s})]$ as in (14)

5: end

6: θ = min(subDir$_j$), W = $\Delta^T K_\theta L_\alpha$

7: for k = 1:mIter

8: $v_{k+1} \leftarrow v_k + (1/2\varepsilon\lambda^2\alpha^2)W^T(u_i - Wv_k)$

9: v(x,y) = shrik[v(x,y)] as in (17)

10: end

11: $f_i' = u_i - Wv$

12: until i > N

13: $\mathbf{s}' = IFFST(f')$

Output: $\mathbf{s}'$

EXAMPLES

To validate the proposed method, there are two numerical experiments including synthetic data and field data. Define Signal-to-noise ratio (SNR) to measure the effectiveness of algorithms as

$$\mathrm{SNR} = 10\log_{10}[\|\mathbf{x}\|_2^2/\|\hat{\mathbf{x}} - \mathbf{x}\|_2^2] \ , \tag{25}$$

where $\mathbf{x}$ and $\hat{\mathbf{x}}$ denote the original trace and estimated one, respectively. SNR and visibility are taken as criteria to check out the scheme. Three relative schemes are taken as comparison including DTV denoising, shearlet shrinkage, and FX decon. FX decon is a useful tool using in random noise suppression (Canales, 1984).

There are several parameters used in Algorithm 1. The regularization parameter λ grows as the noise level increases. λ is set to be 0.01 for all the noise-free data and 0.1 for the noisy data in this article. The FFST is used with two scales, 13 subbands (12 for different direction part and one for low frequency). A large scale parameter α improves the result if the dominant direction feature is reliable and there are few components in non-dominated direction. In the article, the value of α varies from 13 to 5 with increasing noise level. The search of dominant direction θ for subband has been discretized into a $\pi/6$ grid. It is sure that fine tuning of the parameter leads to better results. But the results under the current parameter are enough to show the efficiency of the proposed method.

Synthetic data

A geological model with three layers is applied to synthesize the simulated data. The sands are of higher impedance than shale, but halite is the most. The stratigraphic structure sketch map is presented in Fig. 3a. The seismogram is obtained by convolution between reflection coefficient series (Fig. 3b) and wavelet. In this article, a 30-Hz Ricker wavelet is utilized with sample interval 2ms. Part of the simulated seismic trace is plotted in Fig. 3c.

In practice, a seismogram is often distorted by noise, which interferes with the analysis of seismic feature. In the simulated record testing, the Guassian random noise with variance $\sigma^2 = 0.2$ is added into the original signal to examine the performance of the proposed scheme, as shown in Fig. 3d.

As seismic data has a sparse representation in shearlet framework, shearlet shrinkage is taken as a comparison. DTV minimization is used to process the noisy seismic data directly to show the essential of shearlet transform. In

addition to the above-mentioned two methods, FX decon is taken as an outside of wavelet transform approach for comparison. The four schemes are used to process a series of synthetic data with different levels of contamination. The denoising result ROC is shown in Fig. 4. It can be seen that the proposed method is better than the others. At the same time, the combination between shearlet and DTV is more robust against the noise judging from the steepness of the curves.

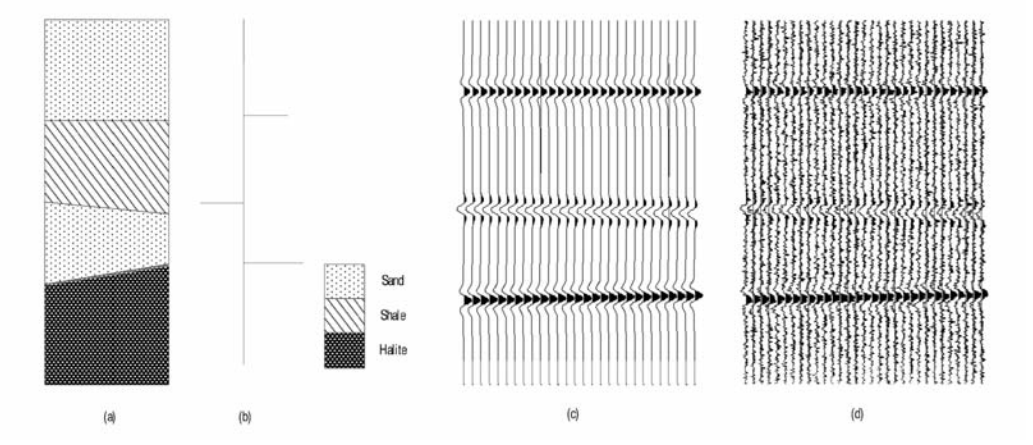

Fig. 3. Simulated seismic record. (a) Synthetic stratigraphic model; (b) reflection coefficient; (c) simulated trace; (d) noisy seismogram with noise variation $\sigma^2 = 0.2$.

From Fig. 4, it is clear that the proposed scheme has a better performance than the others. This is because the proposed method incorporates the advantages of both methods. Natural seismic record contains different direction information. When DTV is used individually to do denoising, it cannot deal with all the direction information as shown in the performance curve.

The result with noise variation $\sigma^2 = 0.2$ is shown in Fig. 3d. It can be concluded that noise is suppressed effectively by shearlet shrinkage as shown in Fig. 5a. However, there are still some non-smooth artifacts left, particularly around the discontinuities. DTV minimization also suppresses the random noise which is obvious in the dominant direction. But when it comes to other direction, the scheme is less effective as seen in Fig. 5b. The FX decon retains many features and removes noise effectively. But it also introduces continuous deviation around 400 ms as shown in Fig. 5c. The fourth method is to use DTV to process each subband. Using the direction information of each subband is our characteristic. The output from the proposed method is shown in Fig. 5d, where the noise is suppressed without bringing in artifacts too much and the features and waveform are held well.

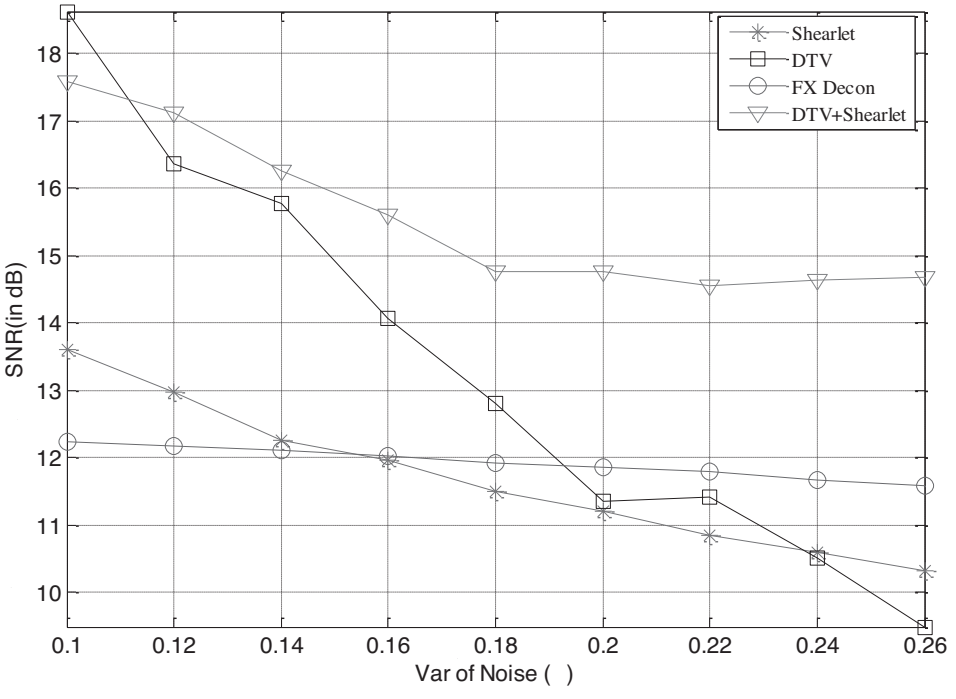

Fig. 4. ROC for denoising SNR with different schemes.

In order to illustrate the result clearly, a randomly selected synthetic trace (19th) is exhibited in Fig. 6. Shearlet shrinkage can individually remove most of the noise, but it also introduces some artifact near singularities as shown in Fig. 6c. When it happened to DTV strategy individually, some artifacts are deduced. But it is not uniform for the direction of edge, which can be an important factor as shown in Fig. 6d. FX decon can also decrease the influence of noise. But the method brings some waves which do not exist in the original data as shown in Fig. 6e. The trace obtained by the proposed method is effective which removes most noise and whose wave structure is preserved very well. In every subband, shearlet extracts one direction component of the seismogram and noise can be uniform and direction free. DTV obtains the direction information and enhances the dominant direction part.

Fig. 7 shows the residual sections corresponding to Figs. 5a-d. There are no obvious original signal components inside as shown in Figs. 7a-d. The proposed method has effectively removed noise without destroying seismic feature.

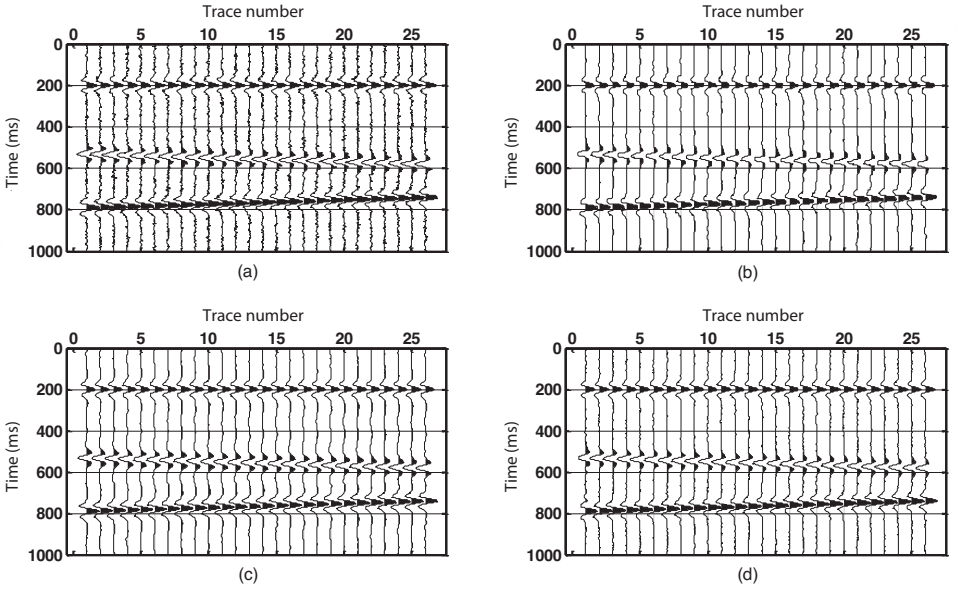

Fig. 5. Denoising results with noise variation (shown in Fig. 3d). Denoised data obtained from shearlet shrinkage, DTV, FX decon and proposed method as shown in (a), (b), (c), (d), respectively.

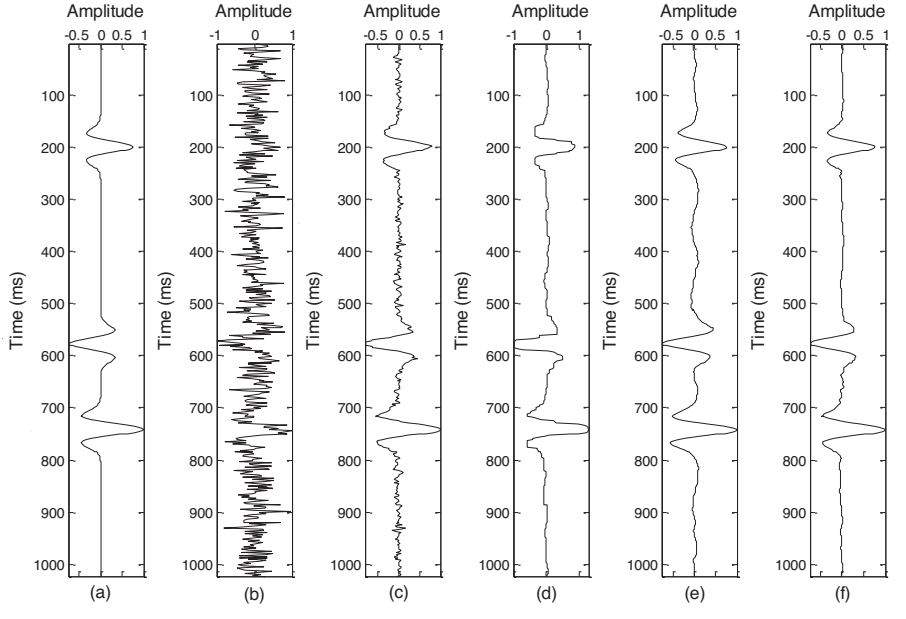

Fig. 6. Single record comparison. (a) Noise free single synthetic data. (b) A noisy version. (c) Single record result by shearlet shrinkage. (d) Single record result by DTV method. (e) Single record result by FX decon. (f) Single record result by proposed method.

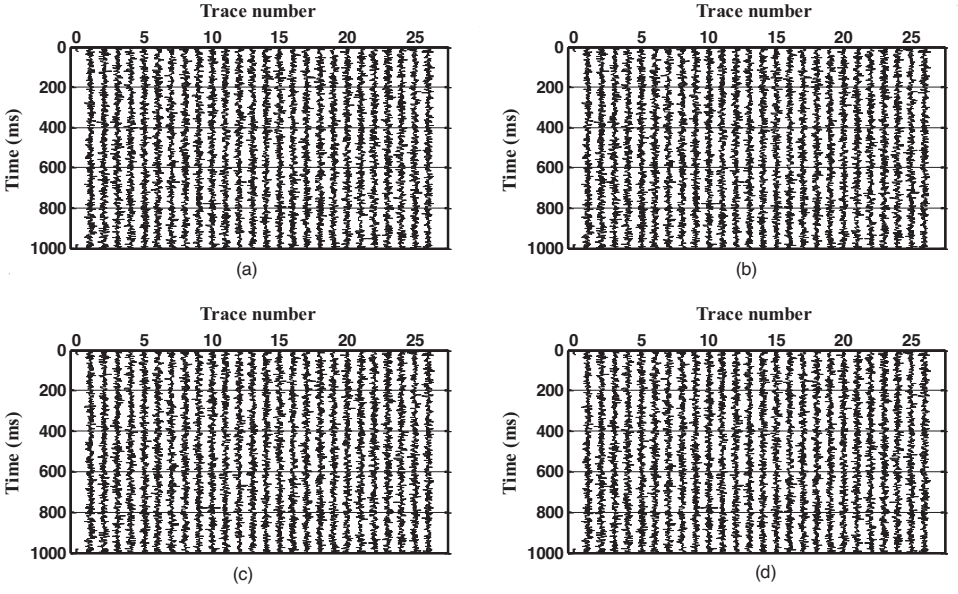

Fig. 7. Difference sections. (a) Difference result by shearlet shrinkage; (b) Difference result by DTV method. (c) Difference result by FX decon. (d) Difference by proposed method.

Field data

The proposed algorithm is also tested for its applicability on field seismic data. The adopted seismic section, shown in Fig. 8a, comes from a portion of some basin area of Sichuan province. It has 512 traces, each consisting of 512 sample points with sample interval 2 ms. This data contains random noise which can be used to confirm the effectiveness of the proposed scheme.

The proposed DTV-synthetic shearlet transform method can suppress noise effectively as shown in Fig. 8b. Two aspects are used to verify that our process has removed noise without eroding strata information. First, the difference between the denoising result and original seismic section is exhibited in Fig. 8c. In the difference section, there is no significant strata structure. It is the evidence that the layer structure is not affected obviously. Secondly, one trace from the section is given, including original signal, its denoising result, and the different between them. They are listed in the left, middle and right of Fig. 8d, respectively. The same conclusion can be reached that the proposed scheme has a good ability to process the seismic data random noise attenuation.

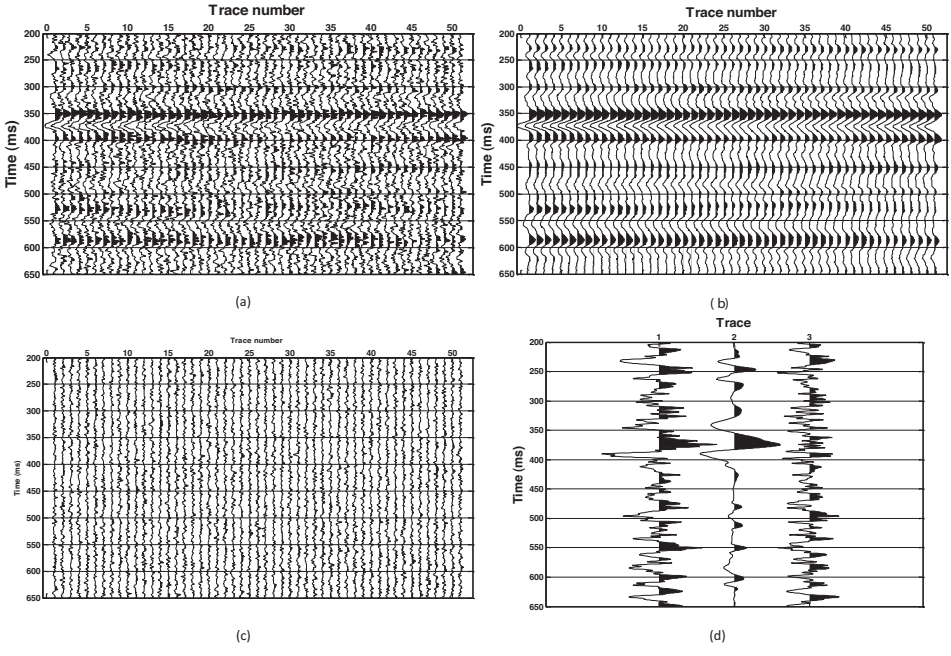

Fig. 8. The field data experiment. (a) Original section; (b) result by proposed method; (c) difference of the original record and the denoised result; (d) signal trace comparison: original trace (left), processed result (middle), difference trace (right).

CONCLUSIONS

In this paper we concentrate on a shearlet-based DTV method for seismic random noise attenuation. Shearlet is an elegant tool for sparse representation of seismic data by decomposing it into several subbands. Each subband has its own dominant direction which helps DTV significantly improve the performance of denoising. This combination gives a new way to take advantages of harmonic analysis and TV. The new method also effectively expands the scope of the application of DTV. Signal with multiple directional characteristics can be processed by this scheme to remove random noise. The numerical experiments with synthetic and field data demonstrate that the proposed method has good performance on random noise suppression and recovers seismic events effectively.

The proposed approach contains several iterations which needs high computational cost. The second aspect is that the statistical characteristics of the noise in the real seismic record are complicated. How to improve the computational efficiency and make the method more practical would be our future work.

ACKNOWLEDGEMENTS

The authors express their gratitude to the editor and the anonymous reviewers for their valuable comments and productive suggestions which have improved the quality of this paper.

This work is supported by the National Science Foundation of China (41274127, 40874066, 41301460).

REFERENCES

Alemie, W. and Sacchi, M.D., 2011. High-resolution three-term AVO inversion by means of a Trivariate Cauchy probability distribution. Geophysics, 76(3): R43-R55.

Bayram, I. and Kamasak, M.E., 2012. Directional total variation. IEEE Sign. Process. Lett., 19: 781-784.

Benning, M., Brune, C., Burger, M. and Müller, J. 2013. Higher-order TV methods-enhancement via Bregman iteration. J. Scientif. Comput., 54: 269-310.

Bredies, K., Kunisch, K. and Pock, T., 2010. Total generalized variation. SIAM J. Imag. Sci., 3: 492-526.

Canales, L.L., 1984. Random noise reduction. Expanded Abstr., 54th Ann. Internat. SEG Mtg., Atlanta.

Do, M.N. and Vetterli, M., 2005,.The contourlet transform: An efficient directional multiresolution image representation. IEEE Transact. Image Process., 14: 2091-2106.

Easley, G.R., Labate, D. and Lim, W., 2008. Sparse directional image representations using the discrete shearlet transform. Appl. Computat. Harmon. Analys., 25: 25-46.

Easley, G.R., Labate, D. and Colonna, F., 2009. Shearlet-based total variation diffusion for denoising. IEEE Transact. Image Process., 18: 260-268.

Figueiredo, M., Bioucas-Dias, J. and Nowak, R., 2007. Majorization-minimization algorithms for wavelet-based image restoration. IEEE Transact. Image Process., 16: 2980-2991.

Guo, K. and Labate, D, 2007. Optimally sparse multidimensional representation using shearlets: SIAM J. Mathemat. Analys., 39: 298-318.

Guo, W., Qin, J. and Yin, W., 2014. A new detail-preserving regularization scheme. SIAM J. Imag. Sci., 7: 1309-1334.

Haghshenas Lari, H. and Gholami, A., 2014. Curvelet-TV regularized Bregman iteration for seismic random noise attenuation. J. Appl. Geophys., 109: 233-241.

Hauser, S. and Steidl, G., 2013. Convex multiclass segmentation with shearlet regularization. Internat. J. Comput. Mathemat., 90: 62-81.

Puryear, C.I. and Castagna, J.P., 2008. Layer-thickness determination and stratigraphic interpretation using spectral inversion: Theory and application. Geophysics, 73(2): R37-R48.

Rudin, L.I., Osher, S. and Fatemi, E., 1992. Nonlinear total variation based noise removal algorithms. Physica D: Nonlinear Phenomena, 60: 259-268.

Shan, H., Ma, J. and Yang, H., 2009. Comparisons of wavelets, contourlets and curvelets in seismic denoising. J. Appl. Geophys., 69: 103-115.

Starck, J.-L., Candès, E.J. and Donoho, D.L., 2002. The curvelet transform for image denoising. IEEE Transact. Image Process., 11: 670-684.

Tang, G. and Ma, J., 2011. Application of total-variation-based curvelet shrinkage for three-dimensional seismic data denoising. IEEE Geosci. Remote Sens. Lett., 8: 103-107.

Yi, S., Labate, D., Easley, G.R. and Krim, H., 2009. A shearlet approach to edge analysis and detection: IEEE Transactions on Image Processing. 18 (5), 929-941.

Yilmaz, O., 2001. Seismic Data Analysis: Processing, Inversion, and Interpretation of Seismic Data. SEG, Tulsa, OK.

Zhong, T., Li, Y., Wu, N., Nie, P. and Yang, B., 2015. Statistical properties of the random noise in seismic data. J. Appl. Geophys., 118: 84-91.